ELSEVIER

Catalysis Today 60 (2000) 21–32

CATALYSIS TODAY

www.elsevier.com/locate/cattod

Methane combustion over low-emission catalytic foam burners

Isotta Cerri, Guido Saracco*, Vito Specchia

Dipartimento di Scienza dei Materiali ed Ingegneria Chimica, Politecnico di Torino, Corso Duca degli Abruzzi, 24-10129 Torino, Italy

Abstract

Fully pre-mixed porous burners, in which methane combustion takes place close to the burner surface are stimulating an increasing interest since they allow lower flame temperatures and NO_x emissions, due to rapid heat removal, thanks to either radiative or convective transfer mechanisms. The present investigation enlightens the further advantages obtainable via the deposition of suitable catalysts onto a porous burner. An industrial ceramic foam support was considered for this purpose: two foam supports were deposited with the $LaMnO_3$-perovskite catalyst, according to two different techniques both based on in situ pyrolysis. For one support (the surface-catalysed burner) the catalyst was deposited, as a thin layer (about 1 mm deep); onto the outlet burner surface (burner-deck), the region where most of the combustion is expected to take place. For the other one (the fully-catalysed burner), the catalyst was deposited within the entire foam matrix. The two catalytic burners and a reference non-catalytic one were comparatively tested in a pilot plant (maximum power of about 30 kW, corresponding to about 1600 kW/m^2). All three burners showed excellent NO_x (<70 ppmv for excesses of air >20%) and HC emissions (<10 ppmv). Conversely, the CO produced at low superficial power (<300 kW/m^2) and excess air (<10%) values was much higher for the non-catalysed burner than for the catalytic ones. Furthermore, the catalyst entailed another positive effect: at the lowest superficial power (190 kW/m^2) it stabilised the combustion towards lower excesses of air, to the benefit of higher thermal efficiency.

Keywords: Catalytic combustion; Methane; Ceramic foam; $LaMnO_3$ perovskite; In situ pyrolysis; Domestic boiler

1. Introduction

Advanced methane combustion systems based on porous media have fast been developing over the last decade in many international research programmes [1–5] for the purpose of enhancing the efficiency of heat transfer with a low environmental impact (reduction of CO_2 and toxic gases, such as CO, HC and NO_x).

The present contribution is inscribed in a wide project aimed at prototyping a low-emission domestic boiler (maximum heat power of about 25 kW) based on a catalytic burner and a sensor-driven pre-mixing apparatus, which is capable of modulating the heat power with a wide turndown ratio (10/1): the minimum power of 2–3 kW, for household heating, and a maximum of about 25 kW to rapidly produce hot water for sanitary purposes. A power modulating system, rather than the on–off regulation one, seems to be the best way of drastically cutting down the number of start-ups and shut-downs which are responsible for undesired pollutant's peaks, quick material degradation (particularly the effects due to creep and thermal shock), and energy loss.

The combustion process in a porous medium is quite different from that which occurs in conventional free flame technology. In a pre-mixed burner, air and methane are mixed through a suitable device and then

* Corresponding author. Tel.: +39-11-564-4654; fax: +39-11-564-4699.
E-mail address: saracco@polito.it (G. Saracco)

0920-5861/00/$ – see front matter
PII: S0920-5861(00)00313-8

fed to the porous panel. Depending on the local momentum of the gaseous mixture, the flame stabilises and in part burns within (radiant regime) or completely outside and over the burner-deck (blue-flame regime). A transition regime also exists, which bridges the previous ones, where the burner-deck is simultaneously covered by blue flames and radiant zones at different locations.

In the radiant regime, because of the large contact area between the gas and solid phases, part of the reaction heat is first rapidly transferred to the solid that glows flamelessly and then, due to the high solid emissivity, to the heat sink by radiation. In such conditions, the flame temperatures within the burner are comparatively low (below 1000°C), to the benefit of low NO_x formation, but to the detriment of the combustion completeness. However, part of the combustion generally occurs just outside the burner, which entails a local increase of temperature and the formation of some NO_x. In this context, the presence of a catalyst is expected to enhance both methane conversion and selectivity towards CO_2, by reducing the kinetics-dependent CO and HC (unburned hydrocarbon) emissions.

By increasing the gas momentum, the flame is partially blown out of the burner-deck until a blue-flame regime is established, which is characterised by a 'carpet' of short blue flames that completely cover the burner-deck. The heat is mainly transferred to the heat sink by convection, which leads to higher flame temperatures, that are responsible for higher NO_x emissions (even though lower than those generated in diffusive flames), but also for negligible HC and CO levels.

Catalytic activation of the burner seems to be a potential way of controlling this trade off, by guaranteeing very low CO and HC emissions even at low flame temperatures. For this purpose, a suitable catalyst should combine good activity towards methane combustion in the temperature range 600–1200°C with high thermal stability. The more active the catalyst, the higher the fraction of the combustion that occurs within the burner. Furthermore, provided the thermal emissivity of the catalyst is higher than that of the support matrix, a stronger heat removal could be achieved to the benefit of even lower flame temperatures within the burner and NO_x emissions.

A series of pioneering attempts to deposit oxidising catalysts on ceramic [6,7] and metallic [8,9] fibre burners with catalysts based on noble metals (such as Pt, Pd) did not lead to satisfactory results in the long period, mainly because the concomitant catalyst sintering, volatilisation and poisoning affected the catalyst activity. Perovskite catalysts ($A_{1-x}A'_xB_{1-y}B'_yO_{3\pm\delta}$, where A, A′=La, Sr, Ba, ... while B, B′=Co, Mn, Cr...) seem to be a favourable alternative to noble metals as they guarantee a higher thermal, chemical and physical stability [10], and a still acceptable catalytic activity. On the basis of some very encouraging results obtained in a previous study, concerning the deposition of $LaMnO_3$ perovskite on a FeCr alloy fibre burner [11], this contribution aims at developing a proper deposition technique of the same catalyst over a ceramic foam and at assessing the catalysed burner performances, mainly in terms of pollutant emissions.

2. Materials and methods

2.1. The ceramic foam

A ceramic foam is a porous material with 'open cavities' within a continuous ceramic matrix, usually processed by a 'polymeric-sponge' replication technique [12]. The polymer carrier, impregnated with a suitable ceramic slurry (composed of finely divided ceramic particles, water and binders) is pyrolysed, thus obtaining a porous ceramic foam, replicating the original polymeric sponge.

The ceramic foam considered in the present study is a 60 ppi (pores per inch) commercial mullite foam, produced by ECO Ceramics bv (Holland) as a porous ceramic substrate for radiant burners, owing to its strong resistance to high-temperature, creep and chemical attack. The disk shaped foam was 12 mm thick and had a 160 mm diameter.

To assess the basic features of the virgin matrix, it was characterised by XRD analysis (PW1710 Philips diffractometer equipped with a monochromator on the diffracted-beam Cu Kα radiation), atomic absorption, SEM observation (SEM 525M with EDAX probe PW9100 by Philips) and permeability measurements.

2.2. Catalyst preparation and characterisation

On the basis of previous studies [13], the $LaMnO_3$ perovskite emerged as the most encouraging catalyst from different perovskite compounds. To check its

compatibility with the support, the preliminary characterisation was carried out on powder-scale samples. The ceramic powder was obtained by grinding the foam samples into sub-micron particles. The obtained powders were then submitted to two different deposition routes. In the first one, the $LaMnO_3$ perovskite was directly deposited on the powder in a variable amount (5–40% b.w.); in the second one, a fixed $LaMnO_3$ percentage (about 40% b.w.) was deposited on the powder, which had previously been coated with La_2O_3 (20–60% b.w.). The inert La_2O_3 phase, which is stable at high temperatures, was tentatively employed to separate the catalyst from the support (thereby preventing possible catalyst deactivation due to catalyst support reactions) and to enhance catalyst dispersion. A modified version of the so-called 'citrate method' [14] was adopted to deposit both the $LaMnO_3$ and the La_2O_3 phases. Stoichiometric amounts of proper precursor salts (mainly nitrates) were mixed with the right amounts of the support powder; about 30% of glycerine (used as a reducing agent) and 100% of water were added to the suspension. The latter was heated to 120°C to generate NO_x and to turn the suspension into a viscous paste. The paste was then rapidly poured into stainless steel vessels and kept in a stove at 180°C. In these conditions, a tumultuous gas generation (mainly NO_x, water vapor and CO_2) occurred, leading to the formation of a solid, very brittle sponge with an exceptional volume. The sponge was milled in an agate mortar and then calcined at 900°C for 24 h. The solid reaction leading to the perovskite crystallisation over the ceramic powders took place during this last treatment.

The physico-chemical structure of each catalyst was characterised (SEM, EDAX, XRD analyses) and the catalytic activity towards methane combustion was measured following temperature-programmed-oxidation (TPO) runs in the same experimental apparatus described in Section 2.4.

2.3. Catalyst deposition techniques

As for the catalytic burners, two catalytic foams were prepared. Taking into account that combustion takes place only in a very thin region near the burner-deck, a catalytic foam with the $LaMnO_3$ coating layer deposited only on the burner-deck was considered. However, since the position and thickness of the flame front within the porous medium are variable, depending on the burner operating conditions, the permeability of the porous medium and the catalyst itself that anticipates ignition [6], a second catalytic burner was prepared in which the $LaMnO_3$ was deposited inside the entire porous foam. Hereafter the former and the latter catalytic foams will simply be referred to as the surface-catalysed and the fully-catalysed burners, respectively. The two catalytic burners were prepared according to different catalyst deposition techniques, both based on the in situ pyrolysis procedure.

For the surface-catalysed foam, a solution containing the precursor salts of the catalyst (nitrates) and glycerine was sprayed onto the burner surface, which had previously been pre-heated at a high temperature (about 700°C). Such a temperature was chosen as the most suitable pre-heating temperature as it was the lowest compromise temperature that led to both nearly complete crystallisation of the $LaMnO_3$ phase, and an acceptable thermal shock, derived from the quenching effect of the sprayed cold solution over the hot foam. After repeated deposition cycles, performed so as to obtain a suitable catalyst load, the foam was finally calcined at 900°C for 4 h.

Conversely, the fully-catalysed burner was obtained by completely impregnating the foam with the same solution, followed by microwave drying. As opposed to conventional drying in electric ovens, microwave drying should in fact guarantee a more homogeneous deposition of the catalyst throughout the entire structure, with no overloading regions close to the foam surface [7]. The microwave drying technique was investigated by varying the $LaMnO_3$ equivalent concentration (calculated as moles of $LaMnO_3$ produced from 1 l of precursor solution) in the 0.2–1 M range and the heating power of the microwave oven in the range 400–3600 kW/m^3 of the sample. The optimisation study was supported by the characterisation of the materials with weight measurement, XRD and SEM observations. This allowed one to find the optimal catalyst deposition conditions: $LaMnO_3$ concentration of the impregnating solution: 0.2 M; power delivered by the microwave oven to the foam: 1000 kW/m^3. Various deposition cycles were repeated before the final calcination step at 900°C for 4 h.

The temperature of the final heat treatment, carried out for the surface-catalysed burner too, was selected

as a compromise between a sufficient catalyst stability (normal burner operating temperatures in the radiant regime are in the range of 600–900°C), and a reasonable specific surface area (negatively affected by sintering phenomena).

Ceramic tablets were prepared in a further set of experiments, which were performed to directly investigate the support as well as the deposited catalyst layer through XRD analysis. The industrial foam was milled into a sub-micron powder, and then isostatically pressed under a load of about 2500 kg/cm^2 to form tablet samples (20 mm in diameter and 2 mm in thickness). The tablets were sintered at 1600°C for 5 h to reach the proper mechanical strength. These well compact and low-porosity tablets were then lined with $LaMnO_3$ according to the in situ pyrolysis technique developed for compact solids and which has been described in detail in a previous work [13].

2.4. Permeability test

Some permeability tests were performed on specific foam disks (50 mm diameter and 12 mm thickness) so as to better characterise the burner. The disks were fully catalysed with different $LaMnO_3$ loads (0–13 wt.%), obtained with a different number of deposition cycles. A fixed specific flow-rate of nitrogen (1 N m^3/(m^2 s)) was forced to pass through the foams at room temperature, and meanwhile the related pressure drop was measured by a U-tube manometer.

2.5. TPO test apparatus

Catalytic activity tests were carried out both on the powder-supported catalysts and on catalytic foam grains (about 2 mm) obtained by grinding the catalysed disks described in Section 2.4. These tests were performed in a TPO apparatus [15].

The TPO equipment consisted of:

- a quartz tubular fixed bed micro-reactor (internal diameter: 3 mm) inserted into a PID controlled oven;
- a mass flow meter delivering synthetic air (21 vol.% of oxygen and 79 vol.% of helium);
- a mass flow meter delivering a methane–helium mixture (10 vol.% of methane and 90 vol.% of helium);
- a thermocouple, inserted into the bed, to measure the bed temperature;
- a thermocouple, to measure the temperature inside the oven;
- a CO_2 FTIR analyser (URAS 10E by Hartmann and Braun) fed with the reactor outlet gases.

As far as the $LaMnO_3$ supported powders are concerned, the catalytic bed contained 0.5 g of the material and was fed with a gas flow-rate of 50 N l/min, with 2 vol.% of methane, 17 vol.% of oxygen and helium as balance. A flow-rate of 10 N l/min of the previous methane–oxygen–helium mixture was used for the $LaMnO_3$ foam grains (total per weight: 0.5 g) placed in the micro-reactor. The lower flow-rate was adopted to allow greater sensitivity of the fixed bed to counterbalance the lower catalyst mass in the bed with the higher gas-phase residence time.

In both cases, the temperature was raised from 25 to 850°C (high enough to allow a complete, even non-catalytic, methane combustion). Then, the temperature was decreased at a 3°C/min rate, meanwhile the same feed flow-rate was delivered and the CO_2 outlet concentration was monitored. The temperature (T_{50}), corresponding to methane half-conversion, was taken as the main index of activity of the examined catalysts.

2.6. The pilot plant for catalytic burner tests

The two catalytic and the non-catalytic burners were tested in the pilot plant (maximum burning rate 30 kW) previously described in [4]. In brief, the fully pre-mixed methane–air mixture was supplied to the panel, which was placed vertically in a water-cooled jacketed combustion chamber, and which was then followed by a shell and tube heat exchanger. A fraction of the exhaust was sampled and delivered to the section analysis: NO_x chemiluminescence analyser, CO and CO_2 infrared analysers, O_2 paramagnetic analyser and HC flame-ionisation detector. A suction pyrometer was inserted to measure the flue gas temperature in the combustion chamber; the latter was also provided with a peep-hole for direct observation of the burner-deck. The composition of the flue gases (CO_2, CO, HC, NO_x expressed as ppmv and referring to dry gases at 0°C, 1013 mbar and for 0% O_2 equivalent concentration) was monitored as a function of the excess air (E_a=0–90%) at different power density values (Q=190–1600 kW/m^2).

3. Results

The XRD pattern of the unsupported ceramic foam powders (Fig. 1a) revealed the presence of mullite ($3Al_2O_3{\cdot}2SiO_2$) and α-alumina (JCPDS card 15-0776 and JCPDS card 46-1212, respectively); a certain gibbosity of the base line could also be seen and this could be ascribed to the presence of an amorphous phase.

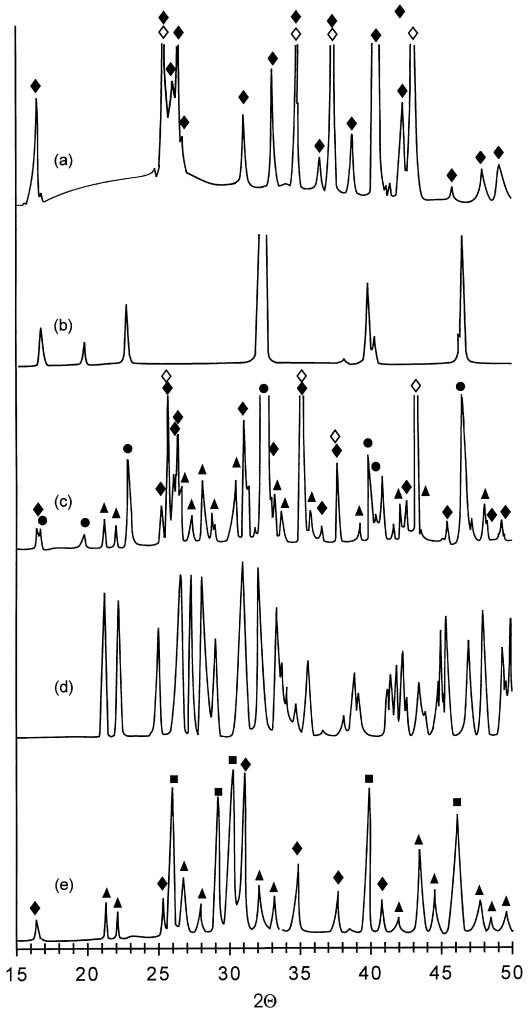

Fig. 1. XRD spectra of powder samples: (a) industrial ceramic foam; (b) pure $LaMnO_3$; (c) $LaMnO_3$ supported on the industrial ceramic powder (20% b.w.); (d) pure $NaLa_9Si_6O_{26}$; (e) La_2O_3 supported on the industrial ceramic powder (20% b.w.). Symbols: (◇) α-alumina; (◆) mullite; (●) $LaMnO_3$; (■) La_2O_3; (▲) $NaLa_9Si_6O_{26}$.

Atomic absorption analysis, aimed at detecting cation impurities in the ceramic support, highlighted the following elements: Na (3.4 wt.%), K (5.58 mg/g), Mg (32.85 μg/g), Li (49.28 μg/g).

Fig. 2 shows the cellular structure of the foam: an incompletely open cell structure can be observed (Fig. 2a) as can a strut with an internal cavity which originally hosted the polymeric strut (Fig. 2b). The average cell and strut diameters are 500–750 μm and 50–100 μm, respectively. EDAX analysis, carried out on both the surface and the cross-section measured the same weight percentage of the main constituting elements.

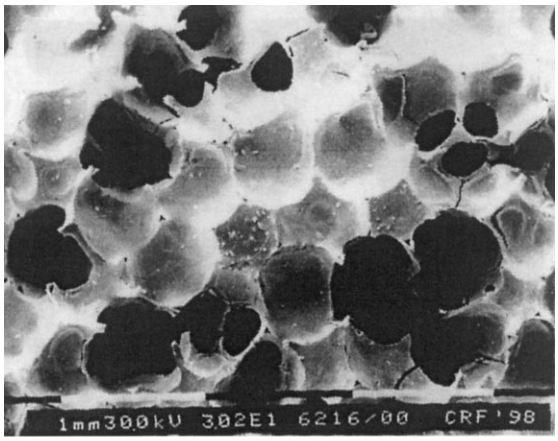

(a)

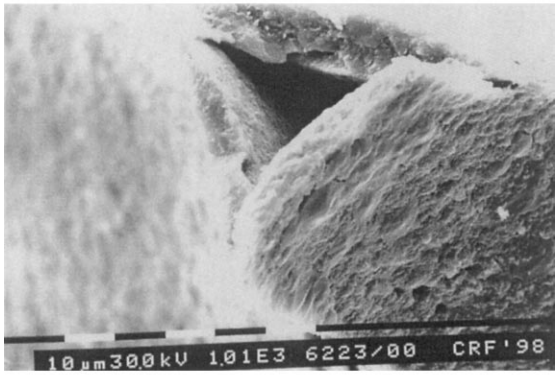

(b)

Fig. 2. SEM micrograph of the industrial ceramic foam: (a) surface; (b) magnification of a bridge.

Figs. 1b–e show the XRD spectra that correspond to pure $LaMnO_3$ (JCPDS card 32-0484), to $LaMnO_3$ (20% b.w.) supported on the industrial ceramic powder, to pure $NaLa_9Si_6O_{26}$ (JCPDS card 32-1109) and to La_2O_3 (20% b.w.) (JCPDS card 40-1281) supported on the industrial ceramic powder, respectively. It is rather clear that, by comparing Fig. 1c with Figs. 1a, b and d, despite some peaks which could not be attributed to any particular substance, the $NaLa_9Si_6O_{26}$ compound can be observed in the supported $LaMnO_3$ catalyst. This compound, a likely reaction product between the lanthanum present in the perovskite and the sodium silicate present in the technical-grade mullite, could also be observed in Fig. 1e, where La_2O_3 was deposited over the mullite instead of the catalyst. La_2O_3 deposition was carried out so as to prepare a stabilised support, on which the perovskite could eventually remain unaffected by the interaction with the support. However, quite surprisingly, the XRD spectra of catalytic tablet samples (not reported here for the sake of briefness) did not show any $NaLa_9Si_6O_{26}$ or even other interaction compounds' peaks.

As for the catalytic activity, Fig. 3 shows methane conversion plots versus temperature (TPO runs) for the $LaMnO_3$ catalyst supported on the ceramic powder at various weight contents (5–40%) as well as for the virgin ceramic material. The increase in the catalyst content resulted in a significant decrease of the temperature required to obtain the same methane conversion.

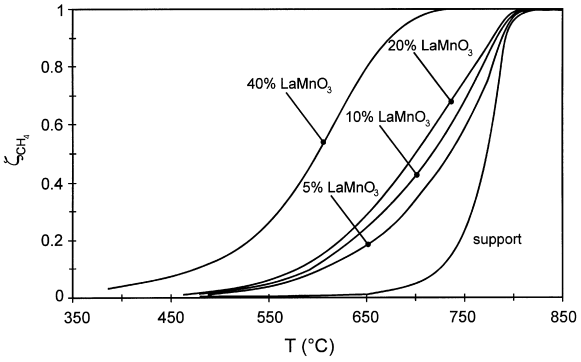

Fig. 3. TPO activity tests towards methane combustion for different amounts of $LaMnO_3$ (0–40% b.w.) deposited on the powders obtained from the industrial ceramic foam.

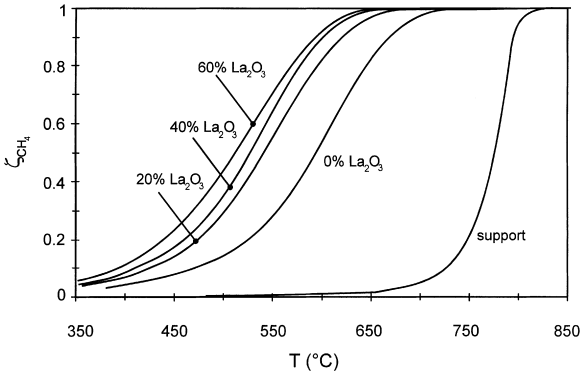

Fig. 4. TPO activity tests towards methane combustion for the $LaMnO_3$ catalyst (40% b.w.) on different La_2O_3-pre-coated ceramic powders (La_2O_3 content: 0–60% b.w.).

In Fig. 4 analogous TPO plots refer to the $LaMnO_3$ catalyst (40% b.w.) supported on ceramic powder pre-coated with different La_2O_3 amounts (0–60% b.w.), together with that corresponding to the pure ceramic support. It can be noticed that La_2O_3 increased the activity of the supported $LaMnO_3$. No significant differences were obtained by varying the La_2O_3 weight content in the 20–60 wt.% range.

The influence of the catalyst amount in fully-catalysed foam samples on the pressure drop (disks) and on the catalytic activity (grains) is shown in Fig. 5.

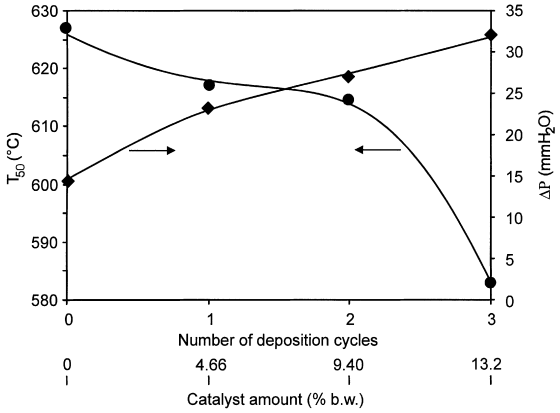

Fig. 5. Influence of the number of $LaMnO_3$ deposition cycles on catalytic activity (T_{50}) and permeability (pressure drop Δp) for fully-catalysed samples (permeating gas: N_2; specific flow-rate: $1\,N\,m^3/(m^2\,s)$; temperature: 25°C).

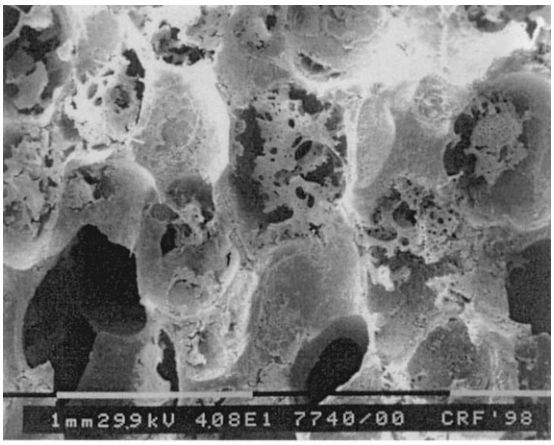

(a)

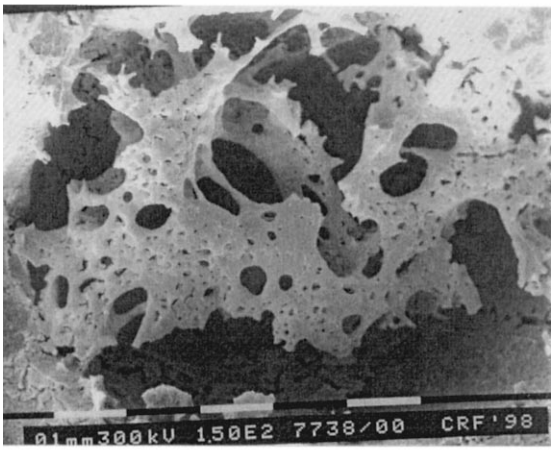

(b)

Fig. 6. SEM micrograph of the fully-catalysed industrial foam: (a) surface (40.8×); (b) magnification of the catalyst structure in a pore (150×).

The distribution of the catalyst inside the foam and the morphology of the catalyst itself (a very porous structure which slightly increases specific surface area) can be seen in Figs. 6a and b, respectively.

Finally, as far as the performance of the three foam burners tested in the pilot boiler (the non-catalytic, the surface-catalysed, the fully-catalysed ones) are concerned, Figs. 7–9 show, respectively, the maps of the combustion regimes, the NO_x and the CO emissions as a function of E_a (2–90%) at various Q values (190–1600 kW/m^2), respectively.

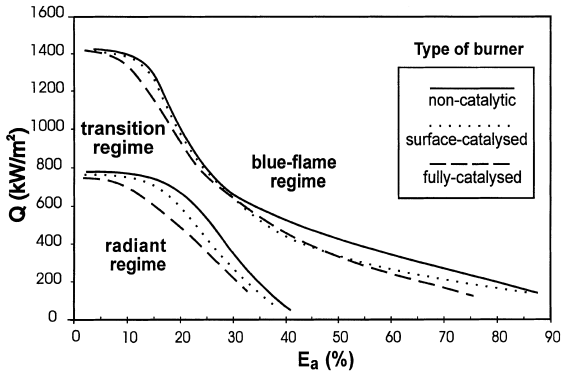

Fig. 7. Map of the combustion regimes as a function of E_a and Q for the three burners: the commercial, surface-catalysed and the fully-catalysed structures.

4. Discussion

As a general feature, ceramic foams have relatively low density, low mass and low thermal conductivity. It can be seen in Fig. 2a that the ceramic network did not have a completely open-cell structure. Some cell entrances were plugged by excess ceramic material. The occurrence of cell-closure reduces permeability, but enhances thermal shock and creep resistance. Under practical domestic boiler applications, the burner is submitted to a high number of on–off cycles; this unfortunately affects the thermo-mechanical resistance, and eventually seriously damages the very brittle foams. For the previously mentioned application, a good thermo-mechanical resistance is a pre-requisite, which is paid for, to some extent, in terms of pressure drop rise. The internal cavity of the struts (Fig. 2b) has shown the usual incomplete shrinkage of the ceramic layer that occurs during polymeric sponge pyrolysis and volatilisation.

SEM observations on both the surface and the cross-section confirmed that the foam is isotropic (i.e. structure and properties have no preferential directionality). As underlined earlier, the EDAX quantitative analysis confirmed a homogeneous composition of the foam, but detected a very high content of silicon, about 48 wt.%, against the stoichiometric content in the mullite (about 30 wt.%), and the presence of mainly sodium and potassium cations. The presence of these cations was also quantitatively confirmed by the atomic absorption. This is not surprising,

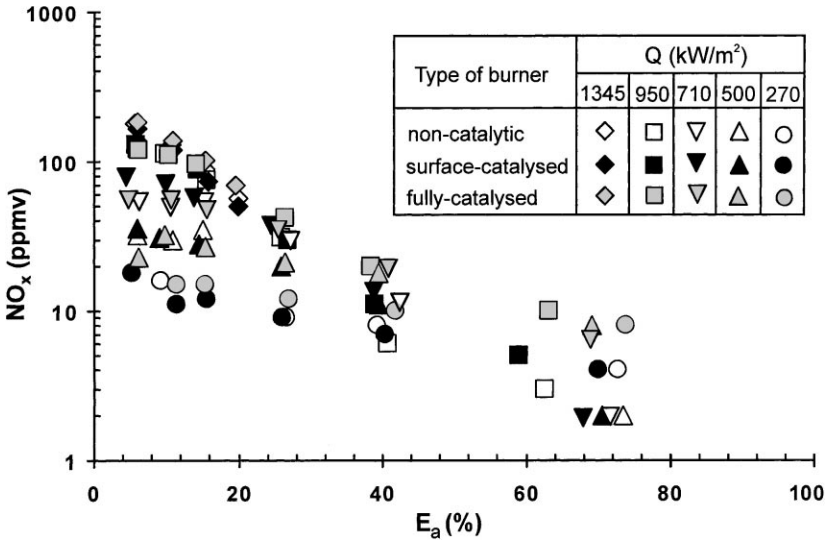

Fig. 8. NO_x emissions as a function of E_a for different Q values for the three ceramic burners: the commercial, surface-catalysed and the fully-catalysed structures.

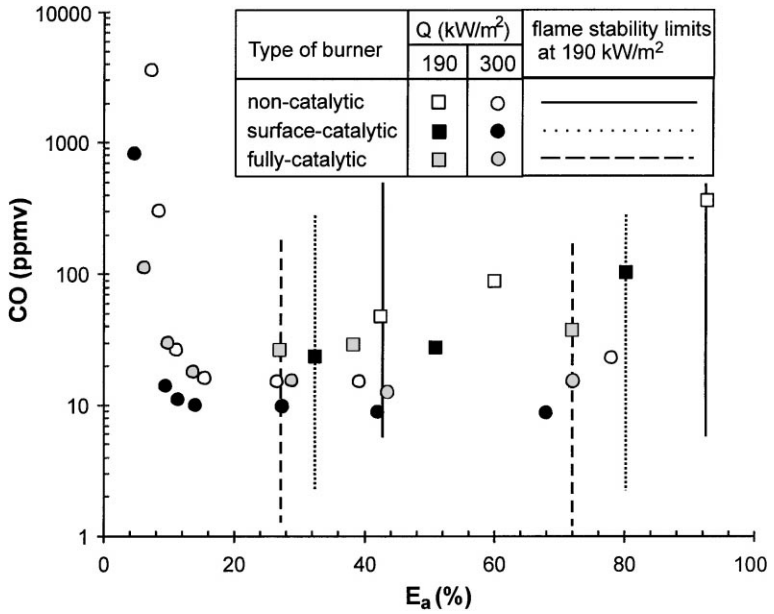

Fig. 9. CO emissions as a function of E_a at Q=190 and 300 kW/m^2 for the three ceramic burners: the commercial, surface-catalysed and the fully-catalysed structures.

since sodium or potassium silicate (as well as e.g. aluminum orthophosphate and magnesium orthoborate) are binders commonly used to process porous ceramics. The role of binders is that of

- providing strength to the ceramic structure after drying;
- preventing collapse during volatilisation of the sponge;
- lowering the mullite sintering temperature to about 1400°C so as to minimise energy consumption for this critical stage.

The addition of the sodium silicate can also partially explain the high amount of silicon found by the EDAX and XRD analyses (the gibbosity of the spectrum in Fig. 1a is compatible with the presence of glassy phases, possibly containing sodium silicate).

The potential reactivity of these binders with the $LaMnO_3$ catalyst to be deposited was a crucial issue. Unfortunately, some reactivity was clearly present. In Fig. 1c, which refers to the $LaMnO_3$-deposited mullite powders, the perovskite and the mullite peaks are evident and confirmed the validity of the preparation route. However, some lanthanum–sodium silicate could also be detected, disclosing that a significant part of the perovskite reacted with sodium silicate. The reactivity of lanthanum with sodium silicate was also confirmed for the La_2O_3-deposited mullite powders (Fig. 1e). That reaction was critical for the catalyst stability not only in powdered samples, where the contact between the catalyst and support is quite intensified, but also at a catalytic burner level; pre-coating of the foam burner with pure La_2O_3 might help to inertise the support prior to $LaMnO_3$ deposition. The lanthanum oxide could in fact convert all the sodium silicate close to the pore walls to be lined, thereby preventing further reaction of the silicate with the catalyst. Moreover, La_2O_3 is completely inert in the presence of the perovskite itself.

TPO tests allowed one to assess that the mullite support is nearly inert towards methane combustion (Fig. 3). However, a low amount of $LaMnO_3$ catalyst (about 5% b.w.) was already capable of improving the activity of the foam. Nonetheless, only a very high content of perovskite ($\geq$40 wt.%) seemed to be necessary to significantly raise the catalytic activity to satisfying values (T_{50}=600°C). The activity of pure $LaMnO_3$ powders, tested in analogous conditions in [12], gave a T_{50} value of about 500°C.

In line with the previous arguments, the interposition of the lanthanum oxide between the catalyst and the ceramic support turned out to be quite a good tool to reduce catalyst deactivation. In Fig. 4 the TPO data obtained for the $LaMnO_3$–La_2O_3-supported ceramic powders have shown that the $LaMnO_3$ activity increased, thanks to the contribution of La_2O_3. The T_{50} values of these samples were always well below 550°C. Furthermore, La_2O_3 does not only hamper the catalyst/support deactivating reaction but it might even enhance the specific surface area of the catalyst, to the benefit of catalytic activity. Since the activity of the various catalysts supported on La_2O_3/mullite powders was not so different above a La_2O_3 content of about 20 wt.%, the latter value might be sufficient to achieve the required inertisation without excessive La_2O_3 consumption.

As already mentioned in Section 2.3, a number of tablet specimens were deposited with the $LaMnO_3$ catalyst. Rather surprisingly, the XRD analysis did not detect the presence of the $NaLa_9Si_6O_{26}$ compound in these samples. $NaLa_9Si_6O_{26}$ was presumably formed at the interface between the mullite tablet and the perovskite layer. However, the amount of this mixed silicate was too low to be detected by XRD analysis. A possible reason for this lies in the lower support–catalyst contact in the tablet samples as opposed to powdered ones. For this reason, at the present primary stage of the research into this type of catalytic burners, it was decided not to carry out a preliminary La_2O_3 inertisation step before catalyst deposition over the foam burners.

According to the previously described methodologies, two catalytic foams were thus prepared: namely, the surface- and the fully-catalysed burners. As far as the fully-catalysed burner is concerned, preliminary attempts were carried out by varying the concentration of the $LaMnO_3$ precursors solution (from 0.2 to 1 M) and the output power (100–900 W) of the microwave oven. The concentration of the solution was found to be a very critical parameter. If, on the one hand, higher concentrations could allow a lower number of deposition cycles to achieve a desired catalyst loading, on the other hand, as checked by SEM observation, concentrations higher than 0.6 M entailed a very bad catalyst dispersion and catalyst–mullite adhesion inside the ceramic foam. During calcination, the large amount of carbonates and nitrates, formerly present in

concentrated precursor solutions, evolved with such a fast reaction that the perovskite being formed could not properly adhere to the pore walls of the foam. The need to have the best possible coating of the burner matrix led to the selection of a concentration value as low as 0.2 M.

Shifting to the optimisation of the microwave-oven power level, it was found that, for values higher than 2500 kW/m^3, the drying was almost immediate (5–10 s). Local hot points inside the foam caused the ignition of the exothermic decomposition of nitrates and carbonates, which contributed to spread pyrolysis all over the matrix. The simultaneous generation of steam and gases was so intense as to push at least part of the solid phase being formed out of the sample. After this intensive drying the foam surfaces were covered with a very brittle brownish solid phase, an amorphous perovskite precursor. On the contrary, powers lower than 800 kW/m^3 required rather long time treatments (about 30 min) to achieve a complete drying, as demonstrated by progressive weight measurements versus time. A power of 1000 kW/m^3 allowed a controlled steam evaporation, prevented rapid pyrolysis of the perovskite precursors, and complete drying was reached within a few minutes (5–10 min).

Various deposition cycles (up to 4) were repeated with the optimised preparation procedure. After 4 cycles the deposited material (exceeding 15 wt.%) was too high to enable good adhesion of all the perovskite crystals to the foam pore walls. For this reason, the pressure drop and catalytic activity were evaluated for foam samples characterised by a number of deposition cycles equal to or lower than three (Fig. 5). As expected, catalytic activity tests and permeability measurements confirmed that an increase of the catalyst amount, on the one hand, enhanced the activity, while on the other, it decreased permeability. Since the pressure drops of the 3-times-deposited burner samples were still acceptable for practical application, the large-scale fully-catalysed burner was prepared for pilot plant testing through three subsequent deposition steps.

The catalyst coating appeared as a very porous structure (Fig. 6). This interesting morphology of the catalyst, derived from the generation of the tumultuous gases that occurred during pyrolysis of the nitrate and carbonate precursors, could, in principle, enlarge the specific surface area of the catalyst that is available for supporting methane combustion.

As far as the preparation of the surface-catalysed burner is concerned, a spray-pyrolysis technique was adopted, as already performed for the activation of metal fibre burners [11]. As mentioned earlier, 0.2 M solution was sprayed onto the hot burner surface (approximately heated to 700°C); three cycles were performed to obtain the surface-catalysed burner. The final pervoskite loading was, in this case, about 3.2 wt.%, as opposed to the 13.2 wt.% of the fully-catalysed burner. The quality and structure of the deposited perovskite catalyst were fully comparable to those of the twin, fully-catalysed burner.

Shifting to the performance of the various burners tested in the pilot boiler, it should first be underlined that the combustion regime extension in the $Q-E_a$ map was somehow affected by the presence of the catalyst (Fig. 7). The catalyst caused a reduction of the radiant regime area and an enlargement of that of the blue-flame regime. As already explained, the flame develops in a dynamic hot space, which is greatly influenced by the local momentum, composition, temperature and the pressure of the reacting gases. The catalyst, affecting both the porosity and the tortuosity of the foam matrix, causes an increase of the pressure drop across the foam as well as of the local momentum of the gas phase. Under the same operating conditions (Q and E_a values) the catalytic burner was thus characterised by a local momentum that was higher than that of the non-catalytic one. This occurrence forced the combustion front downstream, eventually pushing it partially or completely out of the burner at high E_a and Q values.

This effect was only in part balanced by the activity of the catalyst, which should be capable of igniting the combustion further upstream. The restriction of the area corresponding to the radiant regime and the enlargement of that of the blue-flame were obviously more remarkable for the fully-catalysed burner than for the surface-catalysed one.

As a general rule of pre-mixed burners, the heat transferred from the flame to the porous medium, and from this last counterpart to the heat sink, reduces the flame temperature. Since the NO_x formation rate is closely dependent on the gas temperature, higher concentrations can be expected, as observed experimentally (Fig. 8), when operating in the blue-flame

regime with all the burners. As far as the comparison among the three burners on the grounds of NO_x emissions is concerned, the differences were not significant at all. Only at the higher excess air values did the fully-catalysed burner yield NO_x concentrations somewhat higher than those of the other two burners, but however not exceeding 10–20 ppmv. Moreover, since current pre-mixed modulating burners usually work in a restricted E_a range (15–25%), the emissions of all the burners in this range were found to be reasonably good and always lower than 100 ppmv.

As for HC emissions as well as CO emissions (in this last case only for Q>300 kW/m^2), the commercial matrix was characterised by very low concentrations. In particular, the HC outlet concentrations were always lower than 10 ppmv for all the operating conditions. The catalyst did not manage to further reduce these already very low values. Conversely, at low power densities (<300 kW/m^2) and at excess air values <10% or >80%, the CO concentrations for the uncatalysed burner were quite high and unacceptable (Fig. 9). In these conditions the catalyst promoted a significant reduction of the CO levels. Such reduction was more pronounced for the surface-catalysed than for the fully-catalysed one. Presumably, the higher local momentum in the fully-catalysed foam resulted in a lower residence time of the reacting gases in the catalytic-burner.

Moreover, at the lower Q value (190 kW/m^2) it was found that, for the uncatalysed burner, the flame was stable within the excess air range of 43–93%. For E_a values larger than about 93%, the gas momentum was very high which caused the flame to blow out; by decreasing the excess air the flames became stabilised and partially entered the porous media (transition regime), as confirmed by Fig. 7. For E_a values lower than about 43%, it was impossible to keep the burner lit. A likely explanation is that as soon as the combustion front attempted to completely enter the porous media, it was quenched by the very effective radiative heat transfer from the solid. Conversely, the presence of the catalyst stabilised the combustion at lower excess air ranges: 27–72% for the fully-catalysed burner and to 33–80% for the surface-catalysed burner. The catalyst was likely capable of igniting and sustaining the combustion at those low temperatures that are typical of the incipient radiant regime. Hence, the lower limit of the considered E_a range was decreased, compared to the non-catalysed counterpart. On the other hand, the reduced foam permeability entailed by the presence of the catalyst, resulted in a higher gas momentum, which was responsible for the anticipated blow-off (occurring at lower excess air limits than typical ones for the virgin foam burner). The possibility of working steadily in the radiant regime with low noxious gas emissions and at low excess air values allows one to obtain higher thermal efficiency in the boiler. The higher the E_a value, the higher the flue gas flow-rate and consequently the thermal energy loss after the heat exchanger.

5. Conclusions

A ceramic foam burner was catalysed by developing two different techniques in order to deposit the $LaMnO_3$ catalyst either on the outlet surface (the surface-catalysed burner) or entirely on the porous foam structure (the fully-catalysed burner).

The two catalytic burners and their uncatalysed counterparts were tested in a pilot plant of 30 kW maximum power to assess their pollutant emissions. It was found that HC concentrations always remained low for all the tested burners (<10 ppmv). NO_x emissions were not significantly affected by the presence of the catalyst, either. Conversely, the catalyst enabled two prevalent effects:

- it favoured a complete methane combustion to CO_2 at low Q (<300 kW/m^2) and E_a values (<10%) where the CO emissions of the non-catalysed burner were unacceptable;
- it reduced the porosity and permeability of the foams.

The reduction of porosity increased the local momentum of the gases across the foam, causing a reduction of the contact time between the reacting species and the catalyst and forcing the combustion front a little downstream. For this reason, the radiant regime area in the Q–E_a map was shrunk and that for the blue-flame enlarged by the presence of the catalyst. At the same time, the catalyst was able to stabilise combustion at low Q values with lower excess air values to the benefit of higher thermal efficiency.

On the basis of the obtained results, it would seem preferable to use a surface-catalysed foam rather than

a fully-catalysed one, as it is capable of improving burner performance with much lower catalyst loading.

Particular efforts are currently under way to model methane combustion inside the porous catalytic burner, to establish a tool that would be valuable to gain a deeper insight into such a complex structured catalytic reactor and to properly design the burner shape. Long term ageing runs are also being performed to check whether perovskite deactivation takes place through interaction with the support. Thermal fatigue tests are also planned to check the long-term catalyst–support adhesion. In such a case, as discussed earlier, a pre-coating with La_2O_3, prior to $LaMnO_3$ deposition, might be a valuable though expensive solution.

6. Nomenclature

E_a excess of air with respect to stoichiometric conditions (%)
Q specific heat input per unit burner-deck area (kW/m^2)

Acknowledgements

The financial support of Società italiana per il Gas is gratefully acknowledged.

References

[1] S. Moßbauer, O. Pickenäcker, K. Pickenäcker, D. Trimis, Paper presented at the Fifth International Conference on Technologies and Combustion for a Clean Environment, Lisbon, 1999.
[2] R. Viskanta, J.P. Gore, Fourth International Conference on Technologies and Combustion for a Clean Environment; Lisbon, 1997.
[3] V. Khanna, R. Goel, J.L. Ellzey, Combust. Sci. Technol. 99 (1994) 133.
[4] G. Saracco, S. Sicardi, V. Specchia, R. Accornero, M. Guiducci, M. Tartaglino, Gaswärme Int. 45 (1996) 24.
[5] J.A. Gotterba, R.J. Schreiber, R.J. Blair, Paper presented at the Seventh Annual Energy Seminar, Erie, PA, 1985.
[6] J.D. Sullivan, Basic research on radiant burners, Semi-Annual Report, July 1991, GRI Report no. 91/0331, 1991.
[7] A. Bos, E.B.M. Doesburg, C.W.R. Engelen, Paper presented at Eurogel'91, Elsevier, Amsterdam, 1992.
[8] A.J.M. van Wingerden, A.Q.M. Boon, J.W. Geus, Eur. Pat. Appl. (1990) 90202359.7.
[9] F. van Looij, A. Mulder, A.Q.M. Boon, J.F Scheepens, S.W. Geus, Paper presented at the 10th International Congress of Catalysis, Budapest, 1992.
[10] M.F.M. Zwinkels, S.G. Jaras, P. G. Menon, Catal. Rev.-Sci. Eng. 35 (1993) 3, 319.
[11] G. Saracco, L. Cerri, V. Specchia, R. Accornero, Chem. Eng. Sci. 54 (1999) 3605.
[12] J. Saggio-Woyansky, C.E. Scott, W.P. Minnear, Am. Ceram. Soc. Bull. 71 (1992) 11, 1674.
[13] I. Cerri, G. Saracco, F. Geobaldo, V. Specchia, Ind. Eng. Chem. Res. 39 (2000) 24.
[14] F. Abbattista, M. Vallino, in: Proceedings of the First National Meeting of the ASMI, Eng. Mater., 1983.
[15] G. Saracco, G. Scibilia, A. Iannibello, G. Baldi, Appl. Catal. B 8 (1996) 229.